Title:

MpmiR319 promotes gemma/gemma cup formation in the Liverwort *Marchantia polymorpha*

Authors:

Kazutaka Futagami[1]

Masayuki Tsuzuki[1,2]

Yuichiro Watanabe[1]

[1] Department of Life Sciences, Graduate School of Arts and Sciences, The University of Tokyo, Tokyo 153-8902, Japan

[2] Faculty of Agriculture and Marine Sciences, Graduate School of Integrated Arts and Sciences, Kochi University

Correspondence: mtsuzuki@kochi-u.ac.jp (M.Tsuzuki), cyuiwat@g.ecc.u-tokyo.ac.jp (Y.Watanabe)

ORCID

Kazutaka Futagami: https://orcid.org/0000-0002-3321-6508

Masayuki Tsuzuki: https://orcid.org/0000-0002-0642-1143

Yuichiro Watanabe: https://orcid.org/0000-0002-7139-4903

Abstract

Evolutionally conserved miRNA-target mRNA modules have been identified as a core set of functionally and biologically important gene regulation circuits in land plants. Whether the miR159/319 family could maintain such a common biologically fundamental function remains unknown. In this study, we applied the CRISPR-Cas9 system to knock out two Mp*MIR319* loci, *MIR319a* and/or *MIR319b*, in the liverwort *Marchantia polymorpha* to observe phenotypic changes during development. The *MIR319b* knockout line developed fewer gemma cups, while there was a decrease in the number of gemma produced per gemma cup in the *MIR319a* knockout line. It was predicted that miR319 targets Mp*RKD* and Mp*R2R3-MYB21* mRNA and suppresses their expression. To verify this, we constructed miR319-resistant Mp*RKD* (mMp*RKD*) and Mp*R2R3-MYB2*1 (mMp*R2R3-MYB2*1) genes and introduced these genes into wild-type liverwort plants to monitor phenotypic changes. We found that mMp*RKD* induced gemma/gemma cup-less liverworts but mMp*R2R3-MYB2*1 did not. These results indicate that miR319 mainly targets and represses RKD expression rather than that of R2R3-MYB21. Additionally, negative regulation of RKD expression by miR319 controls the placement and number of gemma/gemma cups produced in thalli.

Keywords: *Marchantia*, miR319, gemma, gemma cup, MpRKD

42 **Introduction**

43 It is generally known that plant miRNAs can form complementary base-pair interactions
44 with their target mRNAs with stricter complementarity than their animal counterparts
45 (Rhoades et al., 2002)(Lin and Bowman, 2018). Each plant miRNA can target quite a
46 limited number of mRNAs. Accordingly, target mRNA(s) of each miRNA could be
47 predicted by searching genome sequence data with the aid of the miRNA sequence of
48 interest. *In vivo* studies of miRNAs conserved among land plants have shown that their
49 target mRNAs are also well-conserved cognate genes across phyla (Axtell et al.,
50 2007)(Tsuzuki et al., 2019)(Alaba et al., 2015)(Pietrykowska et al., 2022). Such
51 conserved miRNA-target mRNA modules could be regarded as a core set of functionally
52 and biologically important gene regulation circuits in land plants. But still more
53 experimental data are expected to show the biological significance of highly conserved
54 miRNAs in basal land plants.

55 Among conserved miRNAs, the miR159/319 family has a unique feature in that the
56 miRNA may have changed their target mRNA species during phylogenetic diversification
57 (Palatnik et al., 2007). In Arabidopsis, miR319 preferentially targets mRNAs of
58 *TEOSINTE BRANCHED1, CYCLOIDEA,* and *PROLIFERATING CELL FACTOR (TCP)*
59 genes (Martín-Trillo and Cubas, 2010)(Kosugi and Ohashi, 1997). TCP genes encode
60 bHLH motif transcription factors which affect redundantly cotyledon boundary and form
61 leaf serration (Palatnik et al., 2003)(Koyama et al., 2017).

62 *Marchantia polymorpha* is a liverwort species that stands out as a valuable model for
63 land plant studies, with it garnering an increasing amount of information and resources

64 for comparative evolution studies in recent years (Bowman et al., 2017). Recent studies
65 have revealed that land plants have nearly 300-500 lineage-specific diverse miRNAs
66 (Axtell et al., 2007)(Lin and Bowman, 2018)(Pietrykowska et al., 2022) and that as few
67 as seven miRNA families are deeply conserved from the liverwort *Marchantia*
68 *polymorpha*, the moss *Physcomitrella patens*, to angiosperms (Axtell et al.,
69 2007)(Tsuzuki et al., 2016)(Lin et al., 2016b)(Pietrykowska et al., 2022). But most
70 liverwort miRNAs are yet to be biologically studied in detail enough to obtain a wide
71 understanding of commonality or specificity among land plants.
72 In *M. polymorpha*, it was shown that Mp*miR319* targets the mRNA of MpR2R3-MYB21
73 (an *Arabidopsis* MYB33-like transcription factor, a member of GAMYB families) (Lin
74 et al., 2016b)(Tsuzuki et al., 2016) and that of the RWP-RK DOMAIN (RKD)-containing
75 transcription factor (Lin et al., 2016b) based on data from 5'-RACE or degradome
76 analysis. As such, Mp*miR319* seemingly has some regulatory functions on such target
77 candidate genes, but this has yet to be experimentally tested.
78
79
80 **Materials and methods**
81 *Plant materials and growth condition*
82 Takaragaike-1 (Tak-1, male) and Takaragaike-2 (Tak-2, female) were used as wild-type
83 *M. polymorpha* (Ishizaki et al., 2008). Plants were grown asexually on half-strength
84 Gamborg's B5 medium containing 1% agar, under continuous white fluorescent light at
85 22ºC (Gamborg et al., 1968). For induction of the sexual reproductive phase, plants were

86 grown under a mixture of white fluorescent light and far-red (FR) power light-emitting
87 diodes (OSXXXXT3C1E, OptoSupply; peak emission at 730 nm, with a full width at
88 half-maximum of 20 nm) at 22ºC in continuous light conditions.
89
90 *Genomic DNA*
91 Genomic DNA was extracted from Tak-1 thallus according to the method described in
92 (Tsuzuki et al., 2019) or using the DNeasy Plant Mini kit (QIAGEN, Hilden, Germany).
93
94 *Liverwort transformation and mutant selection*
95 The regenerating thalli method (for *mir319a* or *mir319b* mutants) and G-AgarTrap
96 method (for establishment of gMp*RKD*, mMp*RKD*, gMp*MYB21* and mMp*MYB21* lines)
97 were used for transformation of *M. polymorpha* (Kubota et al., 2013) (Tsuboyama and
98 Kodama, 2018). Briefly, transformed plants were selected on half-strength Gamborg's B5
99 medium containing 0.5 g/L MES, 1% (w/v) agar and 10 μg/ml hygromycin or 0. 5 μM
100 chlorsulfuron, or their combination. After screening T1 plants on drug-supplemented
101 media, we obtained more or less 10 candidate lines for each gRNA in the male and female
102 backgrounds.
103
104 *Plasmid construction to apply CRISPR-Cas9 system*
105 The vectors pMpGE010, pMpGE011 and pMpGE_En03 (Sugano et al., 2018) were used
106 for CRISPR/Cas9-based genome editing of Mp*MIR319A* and Mp*MIR319B* loci. The
107 pMpGE vectors harboring gRNAs targeting *MIR319A* or *MIR319B* genes were

108 constructed as described (Sugano et al., 2018) using oligonucleotide pairs of PAM
109 MIR319a-174f-F and -174f-R, PAM MIR319b-161r-F and -161r-R or PAM-MIR319b-
110 179f-F and -179f-R, respectively, to make pMpGE_En03-gRNA1, pMpGE_En03-
111 gRNA3 and pMpGE_En03-gRNA4 constructs.

112 Selection of *mir319a*^{ge}, *mir319b*^{ge} and *mir319ab*^{ge} mutants was performed as described
113 previously (Tsuzuki et al., 2019). The DNA segments coding *MIR319A* and *MIR319B* loci
114 (with genomic DNA as the template) were amplified using PrimeSTAR HS DNA
115 polymerase (TaKaRa Bio, Kusatsu, Japan) with miR319aF-miR319R or miR319bF-
116 miR319R primer pairs and were sequenced according to Sanger method. PCR and
117 sequencing primer details are listed in Table S1.

118

119 *Introduction of wild-type and miR319 resistant MpRKD/MpR2R3-MYB21 transgenes*

120 The vector pMpGWB300 (Ishizaki et al., 2015) was used to introduce wild-type
121 (gMp*RKD* and gMp*MYB21*) or miR319-resistant types of *RKD* or *MYB21* genes
122 (mMp*RKD* and mMp*MYB21*) into wild-type Tak-1 or Tak-2 lines.

123 To examine the effect of miR319 on repression of MpRKD expression, we generated the
124 pMpGWB300:proMpRKD:MpRKD and pMpGWB300:proMpRKD:mMpRKD
125 plasmids as follows: for pMpGWB300:proMpRKD:MpRKD, the genomic sequence
126 from the Mp*RKD* promoter region (3827 bp upstream from start codon) to the 3'UTR
127 was amplified by PCR with PrimeSTAR HS DNA polymerase (TaKaRa Bio, Kusatsu,
128 Japan) and the primers IF-Hind-pRKD-F and IF-Sal-gRKD-R, using Tak-1 genomic
129 DNA as the template. For pMpGWB300:proMpRKD:mMpRKD, two PCR fragments

130 were amplified from genomic DNA of Tak-1 with the IF-Hind-pRKD-F, Inf-Kpn-gRWP
131 RK-R and IF-Sal-gRKD-R primer sets to mutate the miR319-target sequence in the
132 MpRKD transgene. Each one or two PCR fragments were inserted into pMpGWB300
133 that was cleaved by HindIII and SalI using the In-Fusion Cloning kit (TaKaRa Bio,
134 Kusatsu, Japan) to generate pMpGWB300:proMpRKD:MpRKD and
135 pMpGWB300:proMpRKD:mMpRKD plasmids.
136

137 **Results**

138 *Targeting (perturbation) of either of the two MIR319 genes by guide-RNAs resulted in*
139 *reduced gemma cup production in thalli*

140 *Marchantia polymorpha* has two *MIR319* coding loci, both of which can produce
141 miRNAs of an identical mature sequence, 5'-$_{p}$CUUGGACUGAAGGGAGCUCCC$_{OH}$-3'
142 (Lin et al., 2016b; Tsuzuki et al., 2016). The two *MIR319* loci have now been annotated
143 (*M. polymorpha* genome ver.6.1) as Mp*MIR319A* (Mp3g08965) and Mp*MIR319B*
144 (Mp4g01845), respectively (Fig.1A). To identify the possible biological function(s) of
145 miR319 in *M. polymorpha*, we decided to observe phenotypic changes after knocking
146 down its production. To achieve this, we designed a set of guide RNAs (gRNA 1 for
147 *MIR319A* (Fig.1B) and gRNAs 3 and 4 for *MIR319B* (Fig.1C) to construct vectors to
148 introduce in-del mutations at respective *MIR319* loci by applying the CRISPR/Cas9
149 genome editing system (Sugano et al., 2014)(Sugano et al., 2018).

150 We adopted the *Agrobacterium*-mediated transformation protocol and introduced the
151 vectors into the thalli of Tak-1 to express designed gRNAs and Cas9 (Sugano et al.,

152 2014)(Tsuboyama et al., 2018). After the corresponding drug selection of T1 plants, we
153 amplified respectively targeted genomic sequences from a fraction of T1 thalli and
154 analyzed them by Sanger sequencing. We selected multiple lines that acquired in-del
155 mutations at *MIR319a* or *MIR319b* loci and characterized several of them (Fig. 1B and
156 C) in the following analysis. Mutants with in-del mutations in the Mp*mir319a* locus were
157 characterized as *mir319a*$^{ge-1}$ #5 and *mir319a*$^{ge-1}$#10; mutants with in-del mutations in the
158 Mp*mir319b* locus were characterized as *mir319b*$^{ge-3}$ #11, *mir319b*$^{ge-3}$#15, *mir319b*$^{ge-4}$ #6,
159 and *mir319b*$^{ge-4}$ #9.

160 *Mir319a*^{ge} and *mir319b*^{ge} mutant plants were able to grow as fast as wild-type Tak-1
161 plants. However, we noticed that the mutants – though able to produce gemma cups –
162 developed a smaller number of gemma cups than wild-type plants (Fig. 2); *mir319a*$^{ge-1}$
163 (#5 and #10) and *mir319b*$^{ge-3}$ plants (#11 and #15) produced fewer gemma cups than wild-
164 type liverwort, and *mir319b*$^{ge-4}$ plants produced a significantly lower number (#6 and #9).

165 In addition, we noticed that *mir319a*$^{ge-1}$ (#5 and #10) mutants produced a reduced
166 number of gemma in each gemma cup (Fig.3A). In contrast, *mir319b*$^{ge-3}$ (#11 and #15)
167 mutants produced as much gemma as wild-type plants in each gemma cup (Fig.3A,B).

168 We also created similar *mir319a*^{ge} and *mir319b*^{ge} mutants in female Tak-2 plants.
169 Reduced formation of gemma cups was observed in Tak-2-based mutants as well. Thus,
170 we characterized and report mainly Tak-1 background lines in vegetative growth stages.

171 These observations suggest that miR319 is involved in the formation of gemma and
172 gemma cups in *M. polymorpha* by regulating target gene expression.

173 We also tried to obtain double knock-out miR319ab mutants. To achieve this, we

174 targeted the *MIR319a* locus of *mir319b*$^{ge-3}$ #5 with guideRNA-1. We obtained one
175 double knock-out line and found that the new mutant line acquired a five base deletion in
176 the *MIR319a* locus in addition to a one base addition in the *MIR319b* locus as shown in
177 Fig.1D. For convenience, the line was named *miR319ab*^{ge} *#5/15* mutant (Fig.1D). The
178 severe phenotype of *miR319ab*^{ge}*#5/15* was no more than those of *miR319a* and *mir319b*
179 mutants (Fig.2, #5/15) in terms of the number of developed gemma cups/gemma. The
180 phenotypic severity was expected to be enhanced by disruption of both *miR319a* and *b*
181 loci.
182
183 *Regulation of MpRKD by miR319 is involved in gemma cup formation*
184 Earlier degradome analysis studies indicated that Mp*RKD* (RWP-RK DOMAIN-
185 CONTAINING 1) and Mp*MYB33* mRNAs are targeted by Mp*miR319* (Lin et al., 2016a).
186 Together with the phenotypes of *mir319a*^{ge} and *mir319b*^{ge} mutants, we attempted to
187 address whether these genes are targeted by miR319, with the goal of finding whether
188 susceptibility to miR319 is actually involved in gemma/gemma cup formation in either
189 or both of these mRNA genes.
190 First, we focused on Mp*RKD*. Mp*RKD* encodes an RWP-RK domain-containing
191 transcription factor and was earlier characterized as an evolutionarily conserved regulator
192 of germ cell differentiation (Koi et al., 2016)(Rövekamp et al., 2016). At that time,
193 although not clearly stated, it was reported that Mp*RKD* is expressed on gemma cup rims
194 (Koi et al., 2016) and is necessary for normal growth of cups (Rövekamp et al., 2016).
195 We first tried to test whether Mp*RKD* downregulation by miR319 is linked to

196 gemma/gemma cup formation.

197 We constructed a mutated *RKD* coding sequence which can escape from miR319 action.
198 The 21-nt sequence stretch complementary to miR319 starts from 4 nt downstream its
199 stop codon in the *M. polymorpha RKD* (Mp*RKD*) mRNA. We constructed a miR319-
200 resistant form of the Mp*RKD* gene (designated mMp*RKD*; Fig.4A) by introducing 12
201 base substitutions to decrease the base complementarity. The mMp*RKD* gene was placed
202 downstream its own original 3.8 kbp promoter sequences in the pMpGWB300 vector
203 (Ishizaki et al., 2015). As a control we cloned wild-type Mp*RKD* (designated gMp*RKD*)
204 in the same vector. gMp*RKD* and mMp*RKD* genes were respectively introduced into Tak-
205 1 wild-type plants to obtain gMp*RKD* and mMp*RKD* lines.

206 Both gMp*RKD* and mMp*RKD* line plants showed similar thalli growth rates. But the
207 mMp*RKD* plants showed a striking phenotype in that they did not develop any gemma
208 cups (Fig. 5: mMpRKD). The gemma cup-less phenotypes were similar to *mir319a*$^{ge-1}$,
209 or *miR319ab #5/15* mutants (Fig.5; ab #5/15) in regards to low frequency of gemma cup
210 formation. In contrast, the gMp*RKD* lines produced as many gemma cups as wild-type
211 Tak-1 liverworts (Fig.5; gMpRKD). These results substantiated that the sequences
212 complementary to Mp*miR319* in Mp*RKD* mRNA are deeply involved in gemma/gemma
213 cup formation. This is likely to be related to subsequent suppression of MpRKD
214 translation.

215 As mentioned before, the miR319 target sequence is located in the 3' untranslated region
216 downstream the RKD termination codon sequence. Thus, we were able to design another
217 type of miR319-insensitive *RKD* gene, named Mp*RKD*-Δ3'UTR, by removing the

218 complementary sequences from the 3'-UTR without disturbing RKD translation (Fig.S1-
219 A). When we introduced the insensitive form of Mp*RKD*-Δ3'UTR gene into liverwort,
220 thalli grew but could develop few gemma cups, as was the case with the above mMP*RKD*
221 liverwort (Fig.S1-B).
222
223 *miR319-resistant MpMYB21 did not disturb gemma cup/gemma formation*
224 Mp*MYB21* gene is also a target candidate gene of miR319 on the basis of 5'-RACE or
225 degradome analysis (Tsuzuki et al., 2016)(Lin et al., 2016b). To test whether *MYB21*
226 regulation by miR319 is involved in gemma cup formation, we created a miR319-
227 resistant Mp*MYB21* (mMp*R2R3-MYB21*) gene under its own promoter as we did with the
228 Mp*RKD* gene (Fig.4B). Wild-type, or miR319-sensitive form of Mp*MYB21* (gMp*R2R3-*
229 *MYB21*) gene was also constructed in parallel.
230 *gMYB21* and *mMYB21* genes were introduced into Tak-1 wild-type liverwort to obtain
231 respective transgenic lines. *mMYB21* liverwort lines produced thalli slightly thinner than
232 *gMYB21* lines in width and but could develop gemma cups/gemma without discernible
233 difference in number (Fig.5; mMpMYB21). These results indicated that the Mp*R2R3-*
234 *MYB21* gene has less contribution, if any, than the Mp*RKD* gene in liverwort gemma
235 cup/gemma formation.
236
237 *mMpRKD plants develop deformed antheridiophores/archegoniophores, still with normal*
238 *sperm and egg formation*
239 It was previously reported that Mp*RKD* is expressed in developing eggs and sperm

240 precursors, and regulates egg and sperm formation in *M. polymorpha* (Koi et al.,
241 2016)(Rövekamp et al., 2016). Thus we next checked possible phenotypic changes in
242 germ cell, gametangia and gametangiophore differentiation (Yamaoka et al.,
243 2021)(Shimamura, 2016) in gMp*RKD* and mMp*RKD* liverworts.

244 mMp*RKD* liverworts of Tak-1 background developed male gametophytes under FR
245 illumination (Fig.6C) as early as gMp*RKD* liverworts (Fig.6A). mMp*RKD*
246 antheridiophores had normally-shaped stalked receptables, but with an irregular shape
247 (Fig. 6C,D). Antheridia were formed as if they were protruding outwards but notably not
248 surrounded by antheridiophores in mMp*RKD* lines (Fig.6E,F). We could observe similar
249 sperm mobility in mMp*RKD* liverworts as was found in wild type Tak-1 and gMp*RKD*
250 liverworts.

251 We next checked whether introduction of gMp*RKD* and mMp*RKD* genes into Tak-2
252 wild-type liverworts affects archegonia/archegoniophore development. We established
253 respective transgenic lines using the two constructs described in Fig.4A. mMp*RKD*
254 liverworts of Tak-2 background developed female gametophytes under FR illumination
255 as early as gMp*RKD* liverworts, but they produced archegoniophores with a different
256 shape (Fig.6I) from those of gMp*RKD* (Fig.6G) or Tak-2 plants. mMp*RKD*
257 archegoniophores had short digit shapes but grew normal archegonia (Fig.6I). The
258 archegonia had almost identical appearance (Fig.6J) with those of gMp*RKD* (Fig.6H) or
259 wild-type Tak-2 liverworts.

260

261 **Discussion**

262 While we were profiling *Marchantia* miRNAs after RNA-seq analysis, we tried to
263 induce overexpression of miR319 precursor RNAs to speculate what biological function
264 miR319 might have. Ectopic expression of liverwort miR319 precursor induced
265 abnormal development of gemma cups (Tsuzuki et al., 2016). This suggested that
266 balanced expression of miRNA/target mRNAs is necessary for normal gemma cup
267 development in *M. polymorpha*.

268 The possible function of Mp*RKD* have previously been investigated via mutant
269 analyses in *Marchantia* (Koi et al., 2016)(Rövekamp et al., 2016). It was revealed that
270 Mp*RKD* is essential for normal germ cell differentiation in both male and female
271 gametophytes. Notably, both studies also reported that Mp*RKD* is involved in non-
272 reproductive cells surrounding the antheridia and developing egg and sperm precursors
273 and acts as an essential regulator of germ cell differentiation in *M. polymorpha* (Koi et
274 al., 2016)(Rövekamp et al., 2016). However, it remained uncertain whether biologically
275 significant gene regulatory networks (GRNs) are organized by miR319 and Mp*RKD* and
276 functional at the vegetative stage.

277 It has been described that the founder gemma arise directly from above the center of the
278 apical notch of the thallus, followed by the formation of the cup rims surrounding the
279 gemmae (Shimamura, 2016). Together it was presumed that MpRKD is involved in
280 various stages of cell proliferation to form a variety of tissues in *M. polymorpha*,
281 including gemmae/gemma cups. Our preliminary data showed that the Mp*miR319a*,
282 Mp*miR319b* and Mp*RKD* gene promoters are active in midribs, apical notches and
283 gemma cup areas, which is consistent with recognized phenotypic changes. Still, further

284 investigation is needed to understand how gemma cups are organized by miR319-
285 mediated GRNs.
286 The phenotypes of *mir319b*$^{ge-4}$ #6 and *mir319b*$^{ge-4}$ #9 were more severe than those of
287 *mir319b*$^{ge-3}$ #11 and *mir319b*$^{ge-3}$#15. This difference in severity may have been caused by
288 the position of base changes that occurred inside the miR319 sequence. The *mir319b*$^{ge-4}$
289 plants would be able to produce miRNA, but with differing sequences in the middle
290 portion. Such RNA would not anneal to the target mRNAs effectively and would show
291 more distinct phenotypic changes as indicated in Fig.2.
292
293 In the moss *Physcomitrella patens*, it was found that miR159/319 are encoded in the
294 genome and possibly target cyclin domain proteins and two MYB transcription factors
295 (Axtell et al., 2007). miR159/319 families could be considered as highly conserved
296 miRNAs from bryophytes to angiosperms.
297
298
299 **Acknowledgements**
300 We thank Kohchi, T., Yamaoka, S. of Kyoto University, Ishizaki, K. of Kobe University,
301 Shimamura, M. of Hiroshima University, Nakajima, K. of NAIST for their advice and
302 discussions and Bahari M. for English editing.
303
304 **Author contributions**
305 KF performed the experiments. KF and MT designed the experiments. KF, YW and MT

306 wrote the manuscript.

307

308 **Conflict of interest**

309 The authors declare no conflict of interest.

310

311

312 **Funding**

313 This work was supported by MEXT KAKENHI (21K06225 to Y,W.) and JSPS (Japan

314 Society for the Promotion of Science) funding for Bilateral Joint Research Projects

315 FY2022-23 (JPJSBP 120224601 to Y.W.)

316

317

318 **References**

319 **Alaba S, Piszczalka P, Pietrykowska H, Pacak AM, Sierocka I, Nuc PW, Singh K,**

320 **Plewka P, Sulkowska A, Jarmolowski A, et al** (2015) The liverwort Pellia

321 endiviifolia shares microtranscriptomic traits that are common to green algae and

322 land plants. New Phytol **206**: 352–367

323 **Axtell MJ, Snyder JA, Bartel DP** (2007) Common functions for diverse small RNAs

324 of land plants. Plant Cell **19**: 1750–1769

325 **Bowman JLJL, Kohchi T, Yamato KT, Jenkins J, Shu S, Ishizaki K, Yamaoka S,**

326 **Nishihama R, Nakamura Y, Berger F, et al** (2017) Insights into Land Plant

327 Evolution Garnered from the Marchantia polymorpha Genome. Cell **171**: 287-
328 304.e15
329 **Gamborg OL, Miller RA, Ojima K** (1968) Nutrient requirements of suspension
330 cultures of soybean root cells. Exp Cell Res **50**: 151–158
331 **Ishizaki K, Chiyoda S, Yamato KT, Kohchi T** (2008) Agrobacterium-mediated
332 transformation of the haploid liverwort Marchantia polymorpha L., an emerging
333 model for plant biology. Plant Cell Physiol **49**: 1084–1091
334 **Ishizaki K, Nishihama R, Ueda M, Inoue K, Ishida S, Nishimura Y, Shikanai T,**
335 **Kohchi T** (2015) Development of gateway binary vector series with four different
336 selection markers for the liverwort marchantia polymorpha. PLoS One **10**: 1–13
337 **Koi S, Hisanaga T, Sato K, Shimamura M, Yamato KT, Ishizaki K, Kohchi T,**
338 **Nakajima K** (2016) An Evolutionarily Conserved Plant RKD Factor Controls
339 Germ Cell Differentiation. Curr Biol **26**: 1–7
340 **Kosugi S, Ohashi Y** (1997) PCF1 and PCF2 specifically bind to cis elements in the rice
341 proliferating cell nuclear antigen gene. Plant Cell **9**: 1607–1619
342 **Koyama T, Sato F, Ohme-Takagi M** (2017) Roles of miR319 and TCP transcription
343 factors in leaf development. Plant Physiol **175**: 874–885
344 **Kubota A, Ishizaki K, Hosaka M, Kohchi T** (2013) Efficient Agrobacterium-
345 mediated transformation of the liverwort Marchantia polymorpha using
346 regenerating thalli. Biosci Biotechnol Biochem **77**: 167–172
347 **Lin P-CC, Lu C-WW, Shen B-NN, Lee G-ZZ, Bowman JL, Arteaga-Vazquez MA,**
348 **Liu L-YD, Hong S-FF, Lo C-FF, Su G-MM, et al** (2016a) Identification of

349 miRNAs and their targets in the liverwort Marchantia polymorpha by integrating
350 RNA-Seq and degradome analyses. Plant Cell Physiol **57**: 339–358
351 **Lin P, Lu C, Shen B, Lee G, Bowman JL, Arteaga-vazquez MA, Liu LD, Hong S,**
352 **Lo C, Su G, et al** (2016b) Identification of miRNAs and Their Targets in the
353 Liverwort Marchantia polymorpha by Integrating RNA-Seq and Degradome
354 Analyses Special Focus Issue – Regular Paper. **57**: 339–358
355 **Lin SS, Bowman JL** (2018) MicroRNAs in Marchantia polymorpha. New Phytol **220**:
356 409–416
357 **Martín-Trillo M, Cubas P** (2010) TCP genes: a family snapshot ten years later. Trends
358 Plant Sci **15**: 31–39
359 **Palatnik JF, Allen E, Wu X, Schommer C, Schwab R, Carrington JC, Weigel D**
360 (2003) Control of leaf morphogenesis by microRNAs. Nature **425**: 257–263
361 **Palatnik JF, Wollmann H, Schommer C, Schwab R, Boisbouvier J, Rodriguez R,**
362 **Warthmann N, Allen E, Dezulian T, Huson D, et al** (2007) Sequence and
363 expression differences underlie functional specialization of Arabidopsis
364 microRNAs miR159 and miR319. Dev Cell **13**: 115–25
365 **Pietrykowska H, Sierocka I, Zielezinski A, Alisha A, Carrasco-Sanchez JC,**
366 **Jarmolowski A, Karlowski WM, Szweykowska-Kulinska Z** (2022) Biogenesis,
367 conservation, and function of miRNA in liverworts. J Exp Bot **73**: 4528–4545
368 **Rhoades MW, Reinhart BJ, Lim LP, Burge CB, Bartel B, Bartel DP** (2002)
369 Prediction of plant microRNA targets. Cell **110**: 513–520
370 **Rövekamp M, Bowman JL, Grossniklaus U** (2016) Marchantia MpRKD Regulates

371 the Gametophyte-Sporophyte Transition by Keeping Egg Cells Quiescent in the
372 Absence of Fertilization. Curr Biol **26**: 1782–1789
373 **Shimamura M** (2016) Marchantia polymorpha: Taxonomy, phylogeny and
374 morphology of a model system. Plant Cell Physiol **57**: 230–256
375 **Sugano SS, Nishihama R, Shirakawa M, Takagi J, Matsuda Y, Ishida S, Shimada**
376 **T, Hara-Nishimura I, Osakabe K, Kohchi T** (2018) Efficient CRISPR/Cas9-
377 based genome editing and its application to conditional genetic analysis in
378 Marchantia polymorpha. PLoS One **13**: e0205117
379 **Sugano SS, Shirakawa M, Takagi J, Matsuda Y, Shimada T, Hara-Nishimura I,**
380 **Kohchi T** (2014) CRISPR/Cas9-mediated targeted mutagenesis in the liverwort
381 Marchantia polymorpha L. Plant Cell Physiol **55**: 475–481
382 **Tsuboyama S, Kodama Y** (2018) Highly efficient G-AgarTrap-mediated
383 transformation of the Marchantia polymorpha model strains Tak-1 and Tak-2.
384 Plant Biotechnol **35**: 399–403
385 **Tsuboyama S, Nonaka S, Ezura H, Kodama Y** (2018) Improved G-AgarTrap: A
386 highly efficient transformation method for intact gemmalings of the liverwort
387 Marchantia polymorpha. Sci Rep **8**: 1–10
388 **Tsuzuki M, Futagami K, Shimamura M, Inoue C, Kunimoto K, Oogami T** (2019)
389 An Early Arising Role of the MicroRNA156 / 529- SPL Module in Reproductive
390 Development Revealed by the Liverwort Marchantia polymorpha Report An Early
391 Arising Role of the MicroRNA156 / 529- SPL Module in Reproductive
392 Development Revealed by the Liverwort. Curr Biol **29**: 1–8

393 **Tsuzuki M, Nishihama R, Ishizaki K, Kurihara Y, Matsui M, Bowman JLJL,**
394 **Kohchi T, Hamada T, Watanabe Y** (2016) Profiling and characterization of
395 small RNAs in the liverwort, Marchantia polymorpha, belonging to the first
396 diverged land plants. Plant Cell Physiol **57**: 359–372
397 **Yamaoka S, Inoue K, Araki T** (2021) Regulation of gametangia and gametangiophore
398 initiation in the liverwort Marchantia polymorpha. Plant Reprod. doi:
399 10.1007/s00497-021-00419-y
400
401 **Figure Legends**
402 Fig.1 (A) Primary *MIR319a or b* RNAs are predicted to be transcribed from two
403 annotated loci in the *M. polymorpha* genome. (B) The row wt shows the wild-type
404 *MIR319a* locus sequence and is targeted by gRNA#1. Mutants #5 and #10 were selected
405 for further analysis among obtained in-del mutants. (C) The row wt shows the wild-type
406 *MIR319b* locus sequence and is targeted by gRNA#3 or #4. Mutants #11 and #15 from
407 gRNA#3 treated-pool and mutants #6 and #9 from gRNA#4 treated-pool were selected
408 for further analysis. X in the superscript *ge-x* indicates guide RNA species with which the
409 respective mutant was created. (D) The genomic change of the double knock-out line for
410 *MIR319a* and *b* loci. *MIR319a* locus has a 5-bp deletion and *MIR319b* ha a 1-bp insertion
411 as depicted.
412
413 Fig. 2 (A) Disruption of Mp*MIR319a* and/or *b* genes reduced the numbers of gemma
414 cups. Five plants were analyzed and the means of the numbers of gemma cups per each

415 thallus were shown. For statistical analysis, the analysis of variance followed by Tukey-
416 Kramer's honestly significant difference test was performed. Statistically significant
417 differences are indicated by different lowercase letters ($P < 0.05$). (B) Appearances of
418 respective thalli. Bar = 1 cm. wt: Tak-1 wild-type plant, #5: *miR319a*$^{ge-1}$ #5, #10:
419 *miR319a*$^{ge-1}$ #10, #11: *miR319b*$^{ge-3}$#11, #15: *miR319b*$^{ge-3}$#15, #6: *miR319b*$^{ge-4}$#6, #5/15:
420 *miR319ab* #5/15.
421
422 Fig. 3 Disruption of Mp*MIR319a* and/or *b* genes reduced gemma formation. (A) The
423 number of gemma formed in each gemma cup. wt: Tak-1 wild-type plant, #5: *miR319a*$^{ge-}$
424 ^{1} #5, #10: *miR319a*$^{ge-1}$ #10, #11: *miR319b*$^{ge-3}$#11, #15: *miR319b*$^{ge-3}$#15. *p < 0.05 (Tukey
425 method). (B) Images of single gemma cups. Bar = 1 cm
426
427 Fig. 4 Exon-intron structures of Mp*RKD* and Mp*R2R3-MYB21* genes and target
428 sequence modifications to construct miR319-resistant mMp*RKD* (A) and mMp*R2R3-*
429 *MYB21* (B) genes. gMpRKD (A) and gMpR2R3-MYB21 genes of miR319-sensitive type
430 were also constructed. Vertical bars indicate conventional base-pairing, double dots
431 indicate G-U pairs. AUG and UGA are the initiation and termination codons of the
432 respective open reading frames. 5'UTR and 3'UTR are respective untranslated regions.
433
434 Fig.5 Introduction of miR319-resistant mMpRKD gene but not mMpMYB21 gene
435 resulted in thalli with fewer numbers of gemma cups.
436

437 Fig.6 Introduction of wild-type RKD gene (gMpRKD) induced normal development of
438 gametophytes respectively in Tak-1 (A,B) and Tak-2 (G, H). Introduction of miR319-
439 resistant type mutant RKD gene (mMpRKD) into Tak-1 induced antheridiophores with
440 normally-shaped stalked receptables but with irregular asymmetric shapes and antheridia
441 exposed out of antheridiophores (C,D,E,F). Introduction of mMpRKD into Tak-2 induced
442 archegoniophores with short digit shapes (I), however they retained normal development
443 of archegonia (J).
444
445 Fig. S1 Introduction of wild type RKD and miR319 resistant RKD genes.
446 (A)Wild-type *RKD* (w) and miR319 resistant *RKD* (R) genes were placed under the
447 direction of the promoter of Mp*RKD* gene （pRKD). The sequence segment
448 complementary to miR319 sequences downstream RKD termination codon was deleted
449 to obtain the miR319 resistant *RKD* gene.
450 (B) Phenotypes of growing thalli of transformants to which wild-type (w#1 and w#2)
451 and resistant (r#1 and #2) transgenes were introduced.
452 (C) The numbers of gemma cups were counted per thallus.
453
454

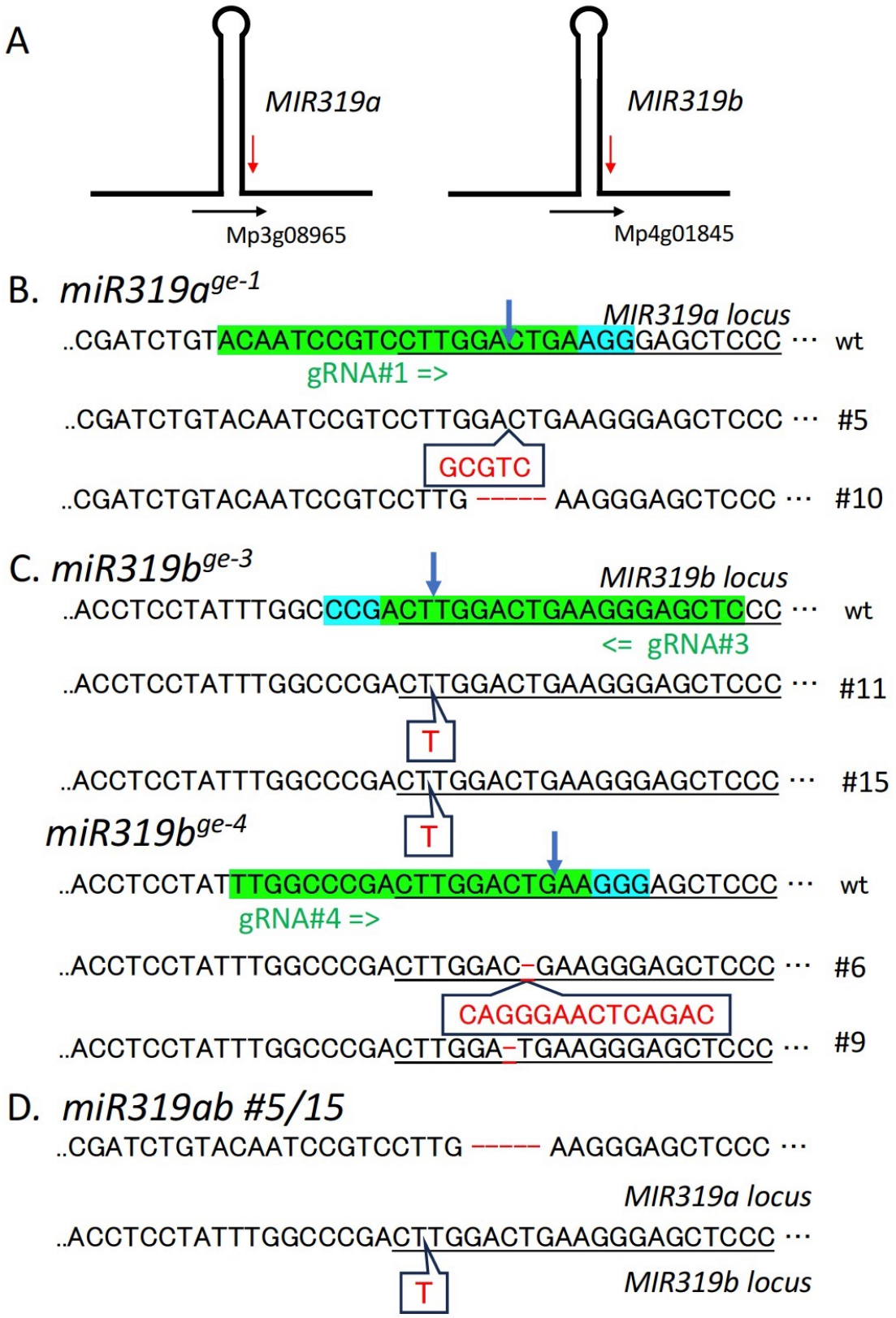

Fig.1 (A) Primary *MIR319a or b* RNAs are predicted to be transcribed from two annotated loci in the *M. polymorpha* genome. (B) The row wt shows the wild-type *MIR319a* locus sequence and is targeted by gRNA#1. Mutants #5 and #10 were selected for further analysis among obtained in-del mutants. (C) The row wt shows the wild-type *MIR319b* locus sequence and is targeted by gRNA#3 or #4. Mutants #11 and #15 from gRNA#3 treated-pool and mutants #6 and #9 from gRNA#4 treated-pool were selected for further analysis. X in the superscript *ge-x* indicates guide RNA species with which the respective mutant was created. (D) The genomic change of the double knock-out line for *MIR319a* and *b* loci. *MIR319a* locus has a 5-bp deletion and *MIR319b* ha a 1-bp insertion as depicted.

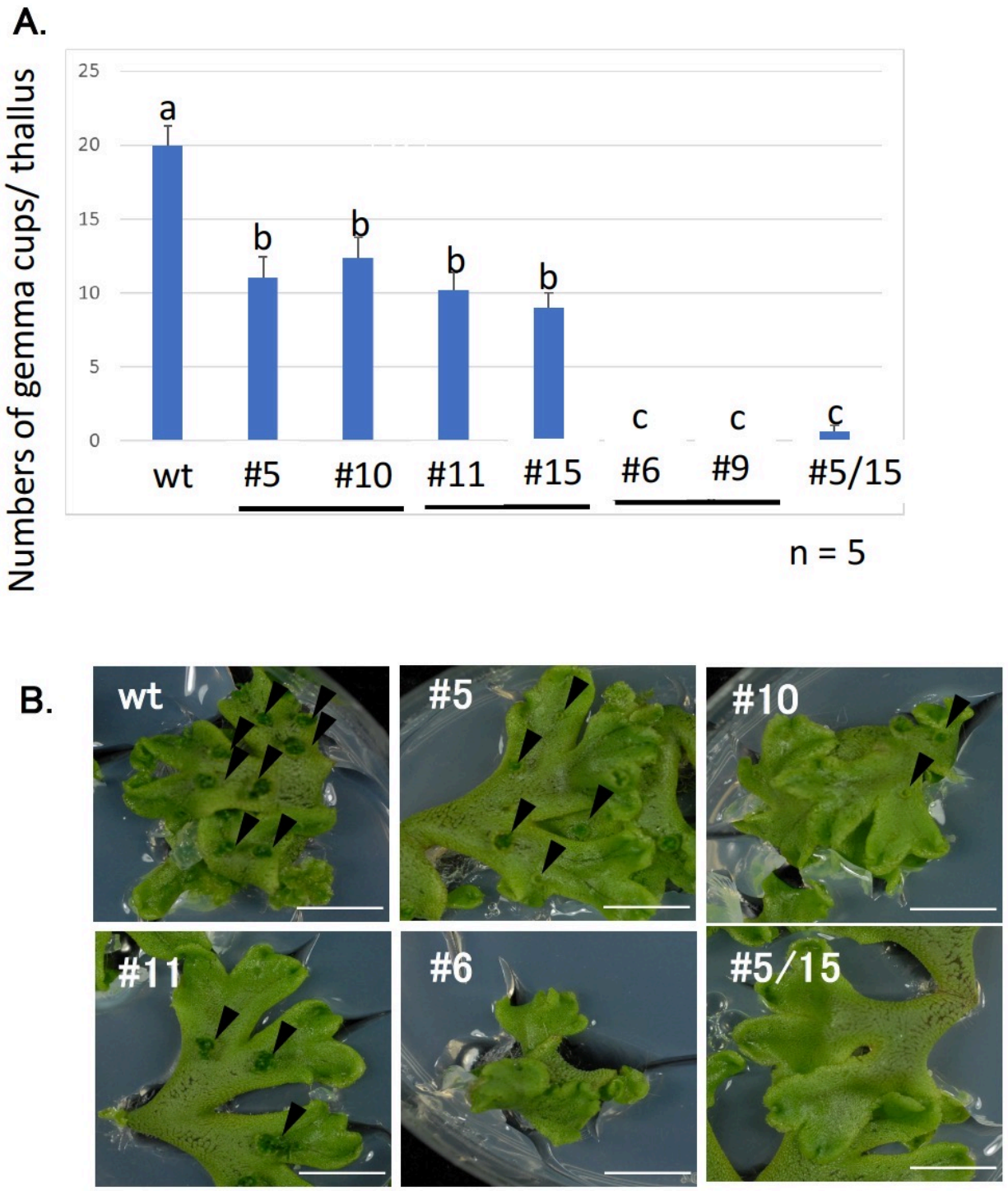

Fig. 2 (A) Disruption of Mp*MIR319a* and/or *b* genes reduced the numbers of gemma cups. Five plants were analyzed and the means of the numbers of gemma cups per each thallus were shown. For statistical analysis, the analysis of variance followed by Tukey-Kramer's honestly significant difference test was performed. Statistically significant differences are indicated by different lowercase letters ($P < 0.05$). (B) Appearances of respective thalli. Bar = 1 cm. wt: Tak-1 wild-type plant, #5: *miR319a*$^{ge\text{-}1}$ #5, #10: *miR319a*$^{ge\text{-}1}$ #10, #11: *miR319b*$^{ge\text{-}3}$#11, #15: *miR319b*$^{ge\text{-}3}$#15, #6: *miR319b*$^{ge\text{-}4}$#6, #5/15: *miR319ab* #5/15.

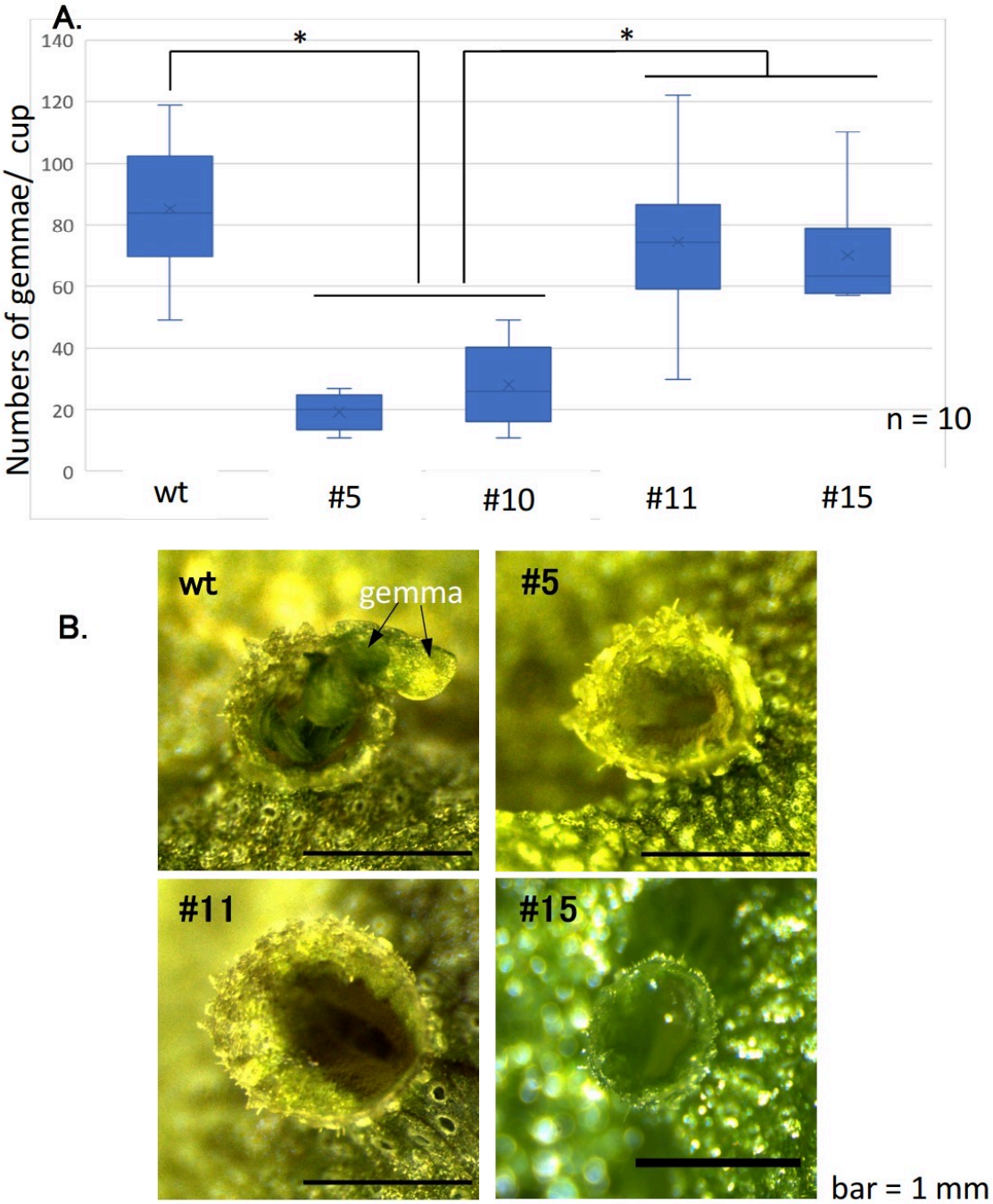

Fig. 3 Disruption of Mp*MIR319a* and/or *b* genes reduced gemma formation. (A) The number of gemma formed in each gemma cup. wt: Tak-1 wild-type plant, #5: *miR319a*$^{ge-1}$ #5, #10: *miR319a*$^{ge-1}$ #10, #11: *miR319b*$^{ge-3}$#11, #15: *miR319b*$^{ge-3}$#15. *$p < 0.05$ (Tukey method). (B) Images of single gemma cups. Bar = 1 cm

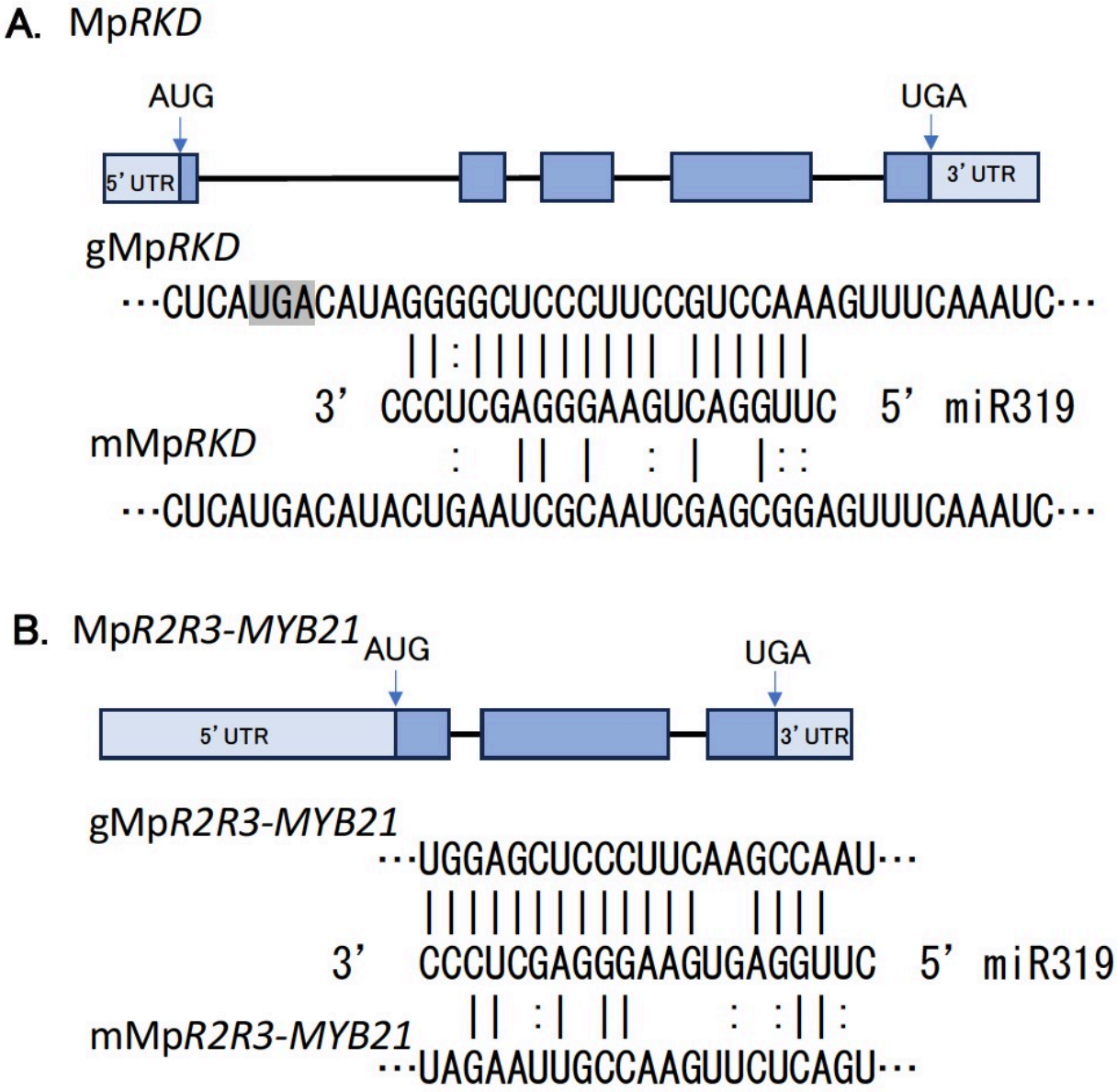

Fig. 4 Exon-intron structures of Mp*RKD* and Mp*R2R3-MYB21* genes and target sequence modifications to construct miR319-resistant mMp*RKD* (A) and mMp*R2R3-MYB21* (B) genes. gMpRKD (A) and gMpR2R3-MYB21 genes of miR319-sensitive type were also constructed. Vertical bars indicate conventional base-pairing, double dots indicate G-U pairs. AUG and UGA are the initiation and termination codons of the respective open reading frames. 5'UTR and 3'UTR are respective untranslated regions.

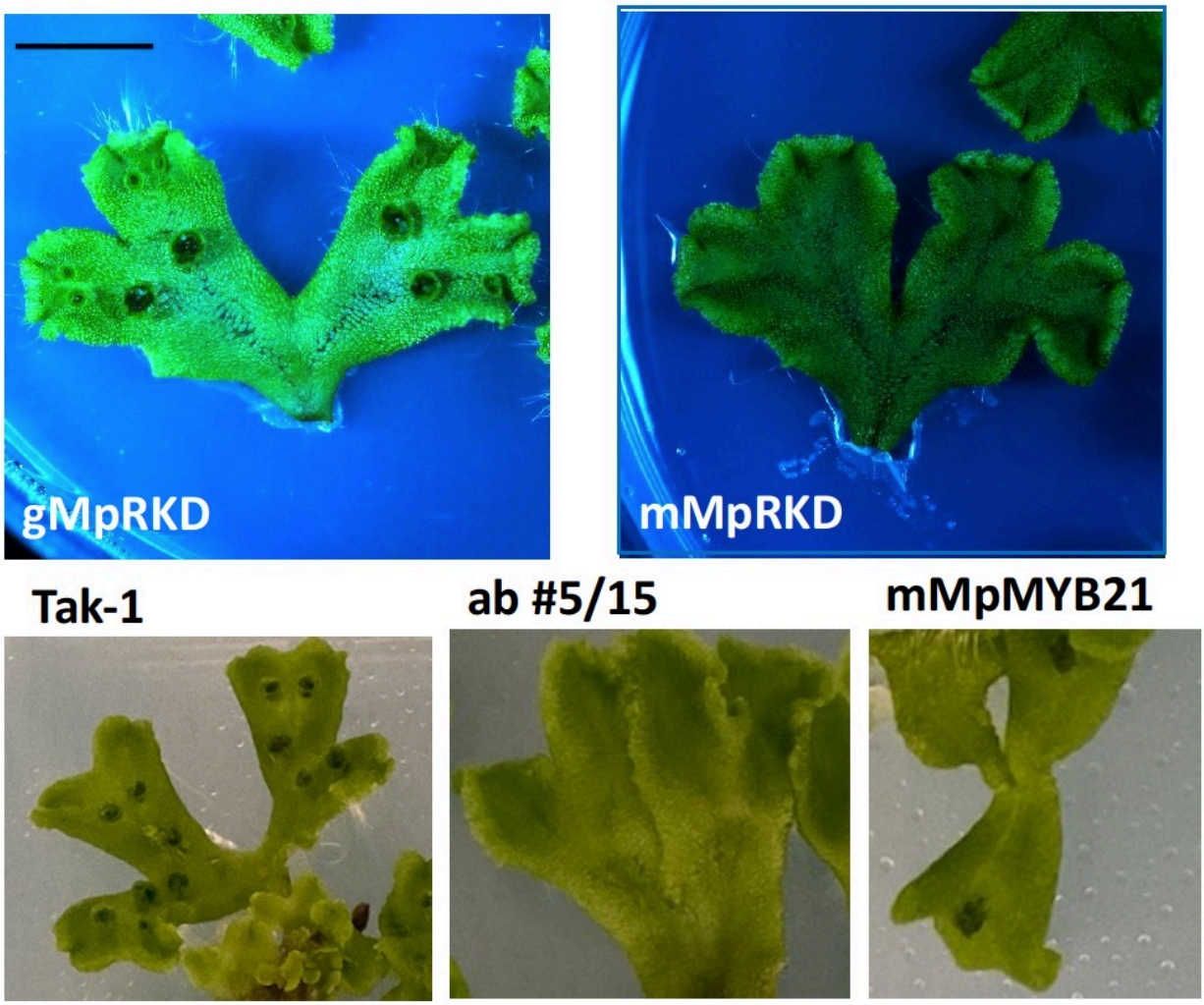

Fig.5 Introduction of miR319-resistant mMpRKD gene but not mMpMYB21 gene resulted in thalli with fewer numbers of gemma cups.

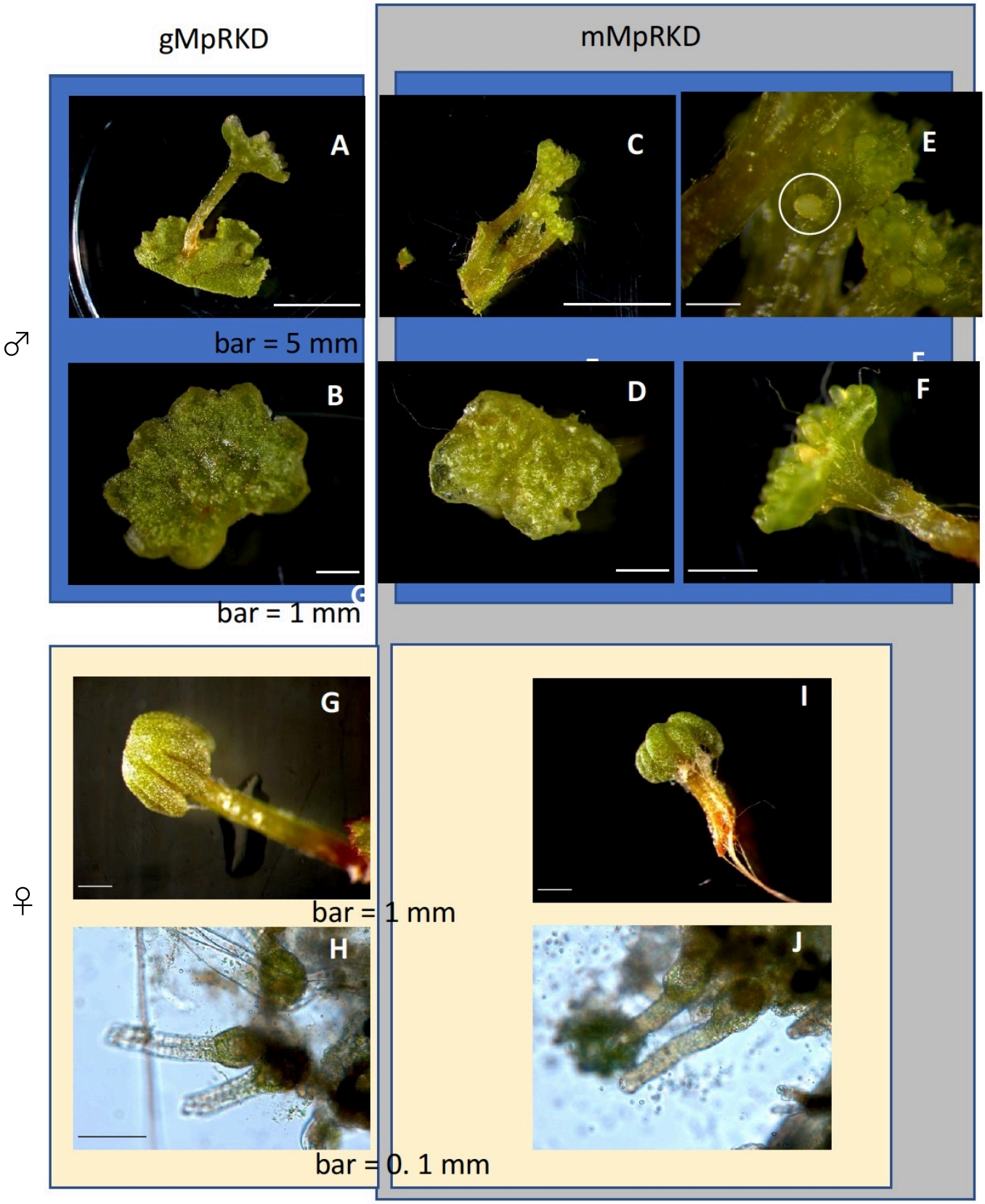

Fig.6 Introduction of wild-type RKD gene (gMp*RKD*) induced normal development of gametophytes respectively in Tak-1 (A,B) and Tak-2 (G, H). Introduction of miR319-resistant type mutant *RKD* gene (mMp*RKD*) into Tak-1 induced antheridiophores with normally-shaped stalked receptables but with irregular asymmetric shapes and antheridia exposed out of antheridiophores (C,D,E,F). Introduction of mMp*RKD* into Tak-2 induced archegoniophores with short digit shapes (I), however they retained normal development of archegonia (J).

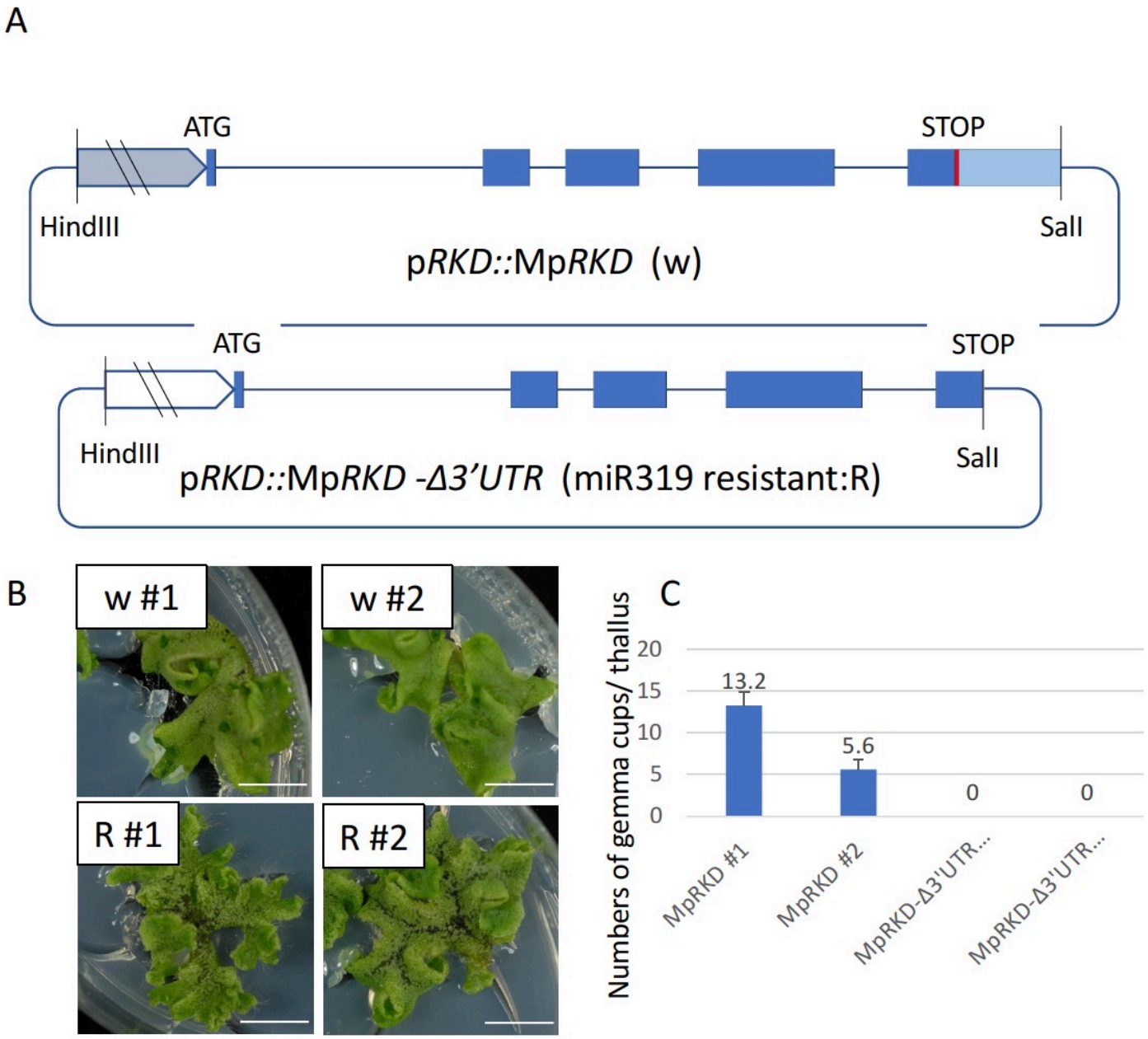

Fig. S1 Introduction of wild type RKD and miR319 resistant RKD genes.

(A)Wild-type *RKD* (w) and miR319 resistant *RKD* (R) genes were placed under the direction of the promoter of Mp*RKD* gene （pRKD). The sequence segment complementary to miR319 sequences downstream RKD termination codon was deleted to obtain the miR319 resistant *RKD* gene.

(B) Phenotypes of growing thalli of transformants to which wild-type (w#1 and w#2) and resistant (r#1 and #2) transgenes were introduced.

(C) The numbers of gemma cups were counted per thallus.

miR319a F	GTTCTGCAGGGACTGTTTTCAGCATCCC	*mir319a* mutant screening
miR319a R	GTTGGTACCTCGACAAGAATTGAGCGAGA	
miR319b F	GTTGTCGACGTGAACTCAGCGCTCATG	*mir319b* mutant screening
miR319b R	GTTGGTACCTACAATCTTTCAAATCAGTACGGAT	
PAM_MIR319a-174f-F	CTCGACAATCCGTCCTTGGACTGA	miR319a gRNA-1
PAM_MIR319a-174f-R	AAACTCAGTCCAAGGACGGATTGT	
PAM_MIR319b-161r-F	CTCGAGCTCCCTTCAGTCCAAGTC	miR319b gRNA-3
PAM_MIR319b-161r-R	AAACGACTTGGACTGAAGGGAGCT	
PAM_MIR319a-166f-F	CTCGCGATCTGTACAATCCGTCCT	miR319a gRNA-2
PAM_MIR319a-166f-R	AAACAGGACGGATTGTACAGATCG	
PAM-MIR319b-179f-F	CTCGTTGGCCCGACTTGGACTGAA	miR319b gRNA-4
PAM-MIR319b-179f-R	AAACTTCAGTCCAAGTCGGGCCAA	
IF-Hind-pRKD-F	ACGACGGCCAGTGCCAAGCTTGGACACCGGAGAGAAATCAA	Mp*RKD* gene construction
IF-Sal-gRKD-R	CGGGGATCCTCTAGAGTCGACTCATGAGACCAGGGTTGAGACAC	
Inf-Kpn-gRWP_RK-R	GGAAATTCGAGCTCGGTACCCGGAAGGTTATGATATCAAGTAGCA	
pMpMIR319a-83F	AGCGGAGAGCATTTCTCAGACC	sequencing of MIR319a promoter
pMpMIR319a-140F	GTCCCCAGACGCATGCAGGTCG	
pMpMIR319a-192F	GGCCGAGCGAGATCCCAGAGAT	
pMpMIR319a-254F	GCCTCGAAACGTAGTGTAGTGT	
pMpMIR319a-315F	CCATGCGCTGTAAGACATGGAC	
pMpMIR319a-375F	TGCGTGACTCTTCCGCATATTT	
pMpMIR319a-423F	TTCAGTCGAGAATGCGATCCCT	
pMpMIR319b-23F	CTGCAAGGCGATTAAGTTGGGT	sequencing of MIR319b promoter
pMpMIR319b-83F	CATTCTCGTACTTTGAACCGTC	
pMpMIR319b-135F	CCAGGTCTCCTTCGCGGAAAAG	
pMpMIR319b-195F	TGGATGCATAGCTTTCCATAAAG	
pMpMIR319b-255F	AGTGGAGATGAGGCGGAGTCAG	
pMpMIR319b-312F	CAAGTCTTCAAGGTGCACTACA	
pMpMIR319b-372F	TAATTGCGCTTGGAAACTACAC	
pMpMIR319b-413F	GTCCATGAGCGCTCATACGTCA	
pRWP_RK-53F	AAATGATACGAAGGAGGTGGACATC	sequencing of MpRKD construct
pRWP_RK-109F	GTGGCAATTTGTCACATTCTTCCAG	
pRWP_RK-162F	GGACGATTGAGCTTACAGAATCTGG	
pRWP_RK-227F	TCGATGGGTTGTGAGAGAACTTGAG	
pRWP_RK-287F	AGACACTAAGCGTGAATTTAGAGGA	
pRWP_RK-336F	AGCCAAAACTACGGACATCTTATTC	
pRWP_RK-395F	AGTGGTTTTCGTTCGGTACAGTCAC	
gRWP_RK-61F	GAATGTGTGGGTGTCACTGGTGGCT	
gRWP_RK-117F	GAATAAGTTTACGACCATGGCTGTA	
gRWP_RK-170F	GTTAGGAAATGTATGTTTCATCCTC	
gRWP_RK-230F	TTGCCGTCTTTAGTCATTGATTCTG	
gRWP_RK-288F	TTATAATTTGGAGATGCGGCTTAGC	
gRWP_RK-350F	TTGTAGCCACGATCTGTCTCCACAA	
gRWP_RK-405F	AGGATTCACGACTAATGGAGAATTC	

Table S1 primers and oligonucleotides used in this study